

Critical behavior in single-crystalline $\text{La}_{0.67}\text{Sr}_{0.33}\text{CoO}_3$

N. Khan, A. Midya, K. Mydeen, P. Mandal, Alois Loidl, D. Prabhakaran

Angaben zur Veröffentlichung / Publication details:

Khan, N., A. Midya, K. Mydeen, P. Mandal, Alois Loidl, and D. Prabhakaran. 2010. "Critical behavior in single-crystalline $\text{La}_{0.67}\text{Sr}_{0.33}\text{CoO}_3$." *Physical Review B* 82 (6): 064422.
<https://doi.org/10.1103/physrevb.82.064422>.

Nutzungsbedingungen / Terms of use:

licgercopyright

Dieses Dokument wird unter folgenden Bedingungen zur Verfügung gestellt: / This document is made available under these conditions:

Deutsches Urheberrecht

Weitere Informationen finden Sie unter: / For more information see:

<https://www.uni-augsburg.de/de/organisation/bibliothek/publizieren-zitieren-archivieren/publiz/>



Critical behavior in single-crystalline $\text{La}_{0.67}\text{Sr}_{0.33}\text{CoO}_3$

N. Khan,¹ A. Midya,¹ K. Mydeen,² P. Mandal,¹ A. Loidl,³ and D. Prabhakaran⁴

¹*Saha Institute of Nuclear Physics, 1/AF Bidhannagar, Calcutta 700064, India*

²*Beijing National Laboratory for Condensed Matter Physics, Institute of Physics, Chinese Academy of Sciences, Beijing 100080, China*

³*Experimental Physics V, Center for Electronic Correlations and Magnetism, Augsburg University, D-86159 Augsburg, Germany*

⁴*Clarendon Laboratory, Department of Physics, University of Oxford, Oxford OX1 3PU, United Kingdom*

(Received 26 May 2010; published 26 August 2010)

The critical behavior of $\text{La}_{0.67}\text{Sr}_{0.33}\text{CoO}_3$ single crystal has been investigated from the bulk magnetization measurements around the Curie temperature (T_C). The detailed analysis of the magnetization indicates the occurrence of a continuous ferromagnetic to paramagnetic phase transition at 223.0 K. The critical exponents $\beta=0.361 \pm 0.007$, $\gamma=1.31 \pm 0.001$, and $\delta=4.64 \pm 0.01$ characterizing this second order phase transition, have been estimated using different techniques such as the Kouvel-Fisher plot, the Arrott-Noaks plot, and critical isotherm analysis. With these values of T_C , β , and γ , one can scale the magnetization below and above T_C following a single equation of state. The consistency in the values of the critical exponents obtained from different methods and the well-obeyed scaling behavior confirm that the calculated exponents are unambiguous and purely intrinsic to the system. These values of the exponents match well with those theoretically predicted for the three-dimensional Heisenberg model with nearest-neighbor interaction.

DOI: [10.1103/PhysRevB.82.064422](https://doi.org/10.1103/PhysRevB.82.064422)

PACS number(s): 75.47.Gk, 71.30.+h, 72.15.Gd

I. INTRODUCTION

Fundamental issues associated with rare-earth cobaltites, $R_{1-x}A_x\text{CoO}_3$ (R =rare-earth ion, A =Ba, Sr, and Ca ion), are the microscopic origin of the magnetism and the nature of the magnetic ground state in these systems. $R_{1-x}A_x\text{CoO}_3$ exhibit very rich and complex magnetic phase diagram due to the occurrence of thermally, compositional, and pressure induced spin-state transition.^{1–20} In LaCoO_3 , Co^{3+} ion is in a low-spin state (t_{2g}^6 , $S=0$) because of the crystal-field splitting being slightly larger than the Hund's coupling energy and undergoes a spin-state transition to either the intermediate-spin ($t_{2g}^5e_g^1$, $S=1$) or the high-spin ($t_{2g}^4e_g^2$, $S=2$) state upon increasing temperature.^{1–3} Sr doping in the parent compound LaCoO_3 generates hole-rich metallic regions in which ferromagnetic (FM) interaction between heterovalent Co^{3+} and Co^{4+} ions sets in with increasing x . Above a critical value of doping $x=0.2$, a FM ground state with metallic conduction is realized in $\text{La}_{1-x}\text{Sr}_x\text{CoO}_3$.^{7–10} It is believed that $\text{La}_{1-x}\text{Sr}_x\text{CoO}_3$ is not a homogeneous ferromagnet but phase separated into hole-rich FM and hole-poor antiferromagnetic regions in microscopic scale even for $x>0.30$.^{1,13} Such microscopic inhomogeneity might affect the cooperative behavior of the Co sublattice, and thereby, the nature of FM to paramagnetic (PM) phase transition. Thus, from the phase transition point of view one may ask whether a true long-range magnetic ordering exists in this system and, if yes, what is the universality class of this magnet.²¹ There are few reports on the analysis of critical behavior on polycrystalline samples of FM cobaltites but no comprehensive understanding exists on either of these issues.^{22–24} An earlier study on $\text{La}_{1-x}\text{Sr}_x\text{CoO}_3$ ($0.2 \leq x \leq 0.3$) samples by Mira *et al.*²² has shown that the FM-PM transition is second order and the value of the critical exponent γ corresponds to a Heisenberg model whereas that of β is mean-field-like. This implies that the system does not belong to a single universality class. Contrary to this, Mukherjee *et al.*²³ have shown that the val-

ues of critical exponents for $\text{La}_{0.5}\text{Sr}_{0.5}\text{CoO}_3$ correspond to those of three-dimensional (3D) Heisenberg universality class. However, another study on the same composition does not support a single universality class— γ is close to the 3D Ising system whereas δ is close to the mean-field one.²⁴

For a true second order phase transition, the critical exponents for a homogeneous magnet should be independent of the microscopic details of the system due to the divergence of correlation length in the vicinity of the transition point and hence their values are almost same for a transition that may occur in different physical systems.²¹ However, the above-mentioned state of affairs in cobaltites have led us to believe that the values of critical exponents determined in polycrystalline materials are strongly affected by the sample quality such as microscopic inhomogeneity and grain-size distribution. Due to the inhomogeneity, polycrystalline samples exhibit a smeared transition with a distribution of T_C 's. This may cause an erroneous determination of the critical exponents. Another source of error is the average size of grains or crystallites in the sample. To determine the intrinsic values of critical exponents or universality class of the magnet, the grain size in the sample should be much larger than the correlation length in the critical region. Hence, one needs a highly homogeneous single crystal to determine the intrinsic values of the exponents. To the best of our knowledge, there is no report on the analysis of critical exponents in single crystals. In order to understand the nature of FM phase transition in rare-earth cobaltites, we present, in this paper, the magnetic properties of high-quality $\text{La}_{0.67}\text{Sr}_{0.33}\text{CoO}_3$ single crystal. The results demonstrate that the temperature (T) and magnetic field (H) dependence of magnetization (M) of single crystal are quite different from those reported for polycrystalline materials. The comprehensive and unambiguous analysis of magnetization data shows that the values of the critical exponents β , γ , and δ estimated using various techniques are in good agreement with those theoretically predicted for 3D Heisenberg model.

II. EXPERIMENTAL TECHNIQUE

The polycrystalline powder sample $\text{La}_{0.67}\text{Sr}_{0.33}\text{CoO}_3$ was prepared by conventional solid-state reaction method using high purity and preheated La_2O_3 , Co_3O_4 and SrCO_3 in appropriate ratio. The mixture was then ground and heated at 1000–1100 °C for few days followed by intermediate grindings. The phase purity of the powder was checked by x-ray diffraction and the sample was found to be of single phase. This powder was then pressed into rods which were used to grow single crystal by the traveling solvent float-zone method using a four-mirror image furnace (Crystal System Inc.) Special attention was paid to achieve the oxygen stoichiometry close to 3. For this reason, the crystal was grown in an oxygen atmosphere at a pressure of 5–9 bar with a typical growth rate 4 mm/h. The crystalline quality and the phase purity were carefully checked by various techniques such as x-ray powder diffraction, Laue diffraction, and electron probe microanalysis. Both electron probe microanalysis and x-ray powder-diffraction data show that the crystal is very pure and stoichiometrically correct. The sharp diffraction spots in neutron Laue pattern indicate the high crystalline quality of the sample and the whole crystal mosaic spread is about 1°. The powder-diffraction patterns can be indexed by a rhombohedral unit cell with the space group $R\bar{3}c$. From the thermogravimetric analysis, we observe that the oxygen content in the present sample is close to 3. The details of synthesis, characterization, structural analysis and transport properties of the present sample are published elsewhere.^{11,25} The dc magnetic measurements were done using a superconducting quantum interference device magnetometer (Quantum Design). The crystal used for the magnetic measurements is a parallelepiped of approximate size $1 \times 2 \times 4$ mm³ and the magnetic field was applied along the longest dimension. The field dependence of magnetization data were collected at 1.0 K intervals over the temperature range from 210 to 242 K. For each $M(H)$ curve, the field was increased from 0 to 5 T and then decreased to 0 again. Prior to measurements, the sample was cooled down in absence of magnetic field from 300 to 210 K and waited for 45 min before taking the field-dependent data. After completing the $M(H)$ isotherm at 210 K, the sample temperature was increased by 1 K to 211 K and again waited for 45 min to achieve the good thermal equilibrium. This process was repeated for the subsequent $M(H)$ measurements. At a given temperature, as many as 50 data have been collected for each M - H isotherm. We did not find any difference in $M(H)$ between increasing and decreasing field. The sharp magnetic transition, the absence of upturn in resistivity at low temperature and the large residual resistivity ratio are the indications of good quality of the sample. In order to calculate the internal magnetic field, the applied field was corrected for demagnetization effect.

III. CRITICAL BEHAVIOR OF THE MAGNETIZATION AND SUSCEPTIBILITY

In the vicinity of a second-order magnetic phase transition with Curie temperature T_C , the existence of a diverging cor-

relation length $\xi = \xi_0 |1 - T/T_C|^{-\nu}$ leads to universal scaling laws for the spontaneous magnetization $M_S(T)$ and initial susceptibility $\chi(T)$. According to scaling hypothesis, the spontaneous magnetization $M_S(T)$ below T_C , the inverse initial susceptibility $\chi_0^{-1}(T)$ above T_C and the measured magnetization $M(H)$ at T_C are characterized by a set of critical exponents β , γ , and δ , respectively. They are defined as²¹

$$M_S(0, T) = M_0 (-\varepsilon)^\beta, \quad \varepsilon < 0, \quad (1)$$

$$\chi_0^{-1}(0, T) = (h_0/M_0)(\varepsilon)^\gamma, \quad \varepsilon > 0, \quad (2)$$

$$M(H, T_C) = A_0(H)^{1/\delta}, \quad \varepsilon = 0, \quad (3)$$

where $\varepsilon = (T - T_C)/T_C$ is the reduced temperature and M_0 , h_0/M_0 , and A_0 are the critical amplitudes. Furthermore, the field and temperature dependence of magnetization in the critical regime obeys a scaling relation which according to scaling hypothesis can be expressed as

$$M(H, \varepsilon) = (\varepsilon)^\beta f_\pm [H/\varepsilon^{(\gamma+\beta)}], \quad (4)$$

where f_+ and f_- are the regular functions for temperatures above and below T_C , respectively.²¹ The scaling Eqs. (3) and (4) predict that $\delta = 1 + (\gamma/\beta)$. In terms of the variable $m \equiv |\varepsilon|^{-\beta} M(H, \varepsilon)$ and $h \equiv |\varepsilon|^{-(\gamma+\beta)} H$, called the scaled or renormalized magnetization and scaled or renormalized field, respectively, Eq. (4) reduces to a simple form

$$m = f_\pm(h). \quad (5)$$

Equation (5) implies that for a true scaling relation with proper selection of β , γ , and δ , the scaled m versus h data will fall onto two different universal curves; $f_-(h)$ for temperature below T_C and $f_+(h)$ for temperature above T_C . This is an important criterion for the accurate and unambiguous values of the critical exponents.

IV. RESULTS AND DISCUSSION

Figure 1(a) depicts the temperature variation of field-cooled magnetization (M_{FC}) and zero-field-cooled magnetization (M_{ZFC}) for $\text{La}_{0.67}\text{Sr}_{0.33}\text{CoO}_3$ single crystal measured at a field of 100 Oe. In the paramagnetic state, M_{FC} and M_{ZFC} do not split from each other, and increase monotonically with decreasing temperature. The nature of T dependence of field-cooled and zero-field-cooled magnetization in the FM state is quite different; M_{FC} continue to increase with decreasing temperature like a Brillouin function while M_{ZFC} decreases slowly with decreasing temperature. The decrease of M_{ZFC} below T_C is much slower as compared to that observed in several polycrystalline samples.^{13,14} The appearance of peak in the ZFC curve just below T_C suggests a competition between different magnetic interactions. For further understanding the nature of the magnetic ground state in this sample, the field dependence of M has been investigated well below T_C . The lower inset of Fig. 1(a) shows that M increases sharply with increasing field and a saturationlike behavior appears at high fields above $H \sim 2$ T with a saturated moment $1.8\mu_B/\text{Co}$ ion. The hysteresis loop is very narrow and the values of coercive field and remanent magnetization

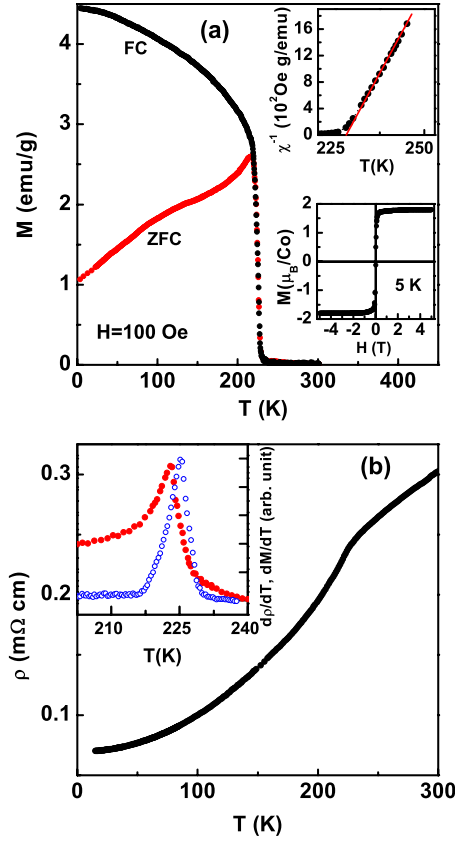


FIG. 1. (Color online) (a) Temperature dependence of field-cooled magnetization (M_{FC}) and zero-field-cooled magnetization (M_{ZFC}) at 100 Oe for $\text{La}_{0.67}\text{Sr}_{0.33}\text{CoO}_3$ single crystal. Lower inset is the hysteresis loop of the magnetization measured at 5 K. Upper inset shows the inverse susceptibility measured at 100 Oe as a function of temperature. The solid line is linear fit to the susceptibility data following the Curie-Weiss law above T_C . (b) Temperature dependence of the resistivity (ρ) for the studied sample. Inset: $d\rho/dT$ (solid symbol) and dM/dT (open symbol) versus temperature.

are quite small, similar to that of typical soft ferromagnets. The $M(H)$ curve reflects a clear difference between magnetic properties of single crystal and polycrystalline samples. Several earlier reports have also shown that the temperature and field dependence of M are quite different for single and polycrystalline samples.^{8–10} For example, magnetization in polycrystalline sample does not saturate but increases linearly with field.¹³ This linear behavior of M has been explained on the basis of coexistence of two magnetic phases, i.e., an inhomogeneous magnetic ground state. According to this model, the system phase separates into hole-rich FM clusters dominated by the FM interaction between heterovalent Co^{3+} and Co^{4+} ions, the clusters being embedded in a hole-poor matrix in which the magnetic interaction is dominated by the antiferromagnetic superexchange between thermally populated high-spin Co^{3+} ($S=2$) pairs interpolated with low-spin Co^{3+} ($S=0$). In such a scenario, instead of saturation, M increases linearly with field due to the presence of Co^{3+} spin with antiferromagnetic interaction.¹³ The absence of linear field dependence of M implies that the amount of hole-poor matrix is negligible in the present sample. Recently, He *et al.*^{17,18} studied comprehensively the specific heat (C_p) and

small-angle neutron scattering (SANS) in $\text{La}_{1-x}\text{Sr}_x\text{CoO}_3$ single crystals for different doping levels in the range $0 \leq x \leq 0.30$. The temperature dependence of specific heat reveals two regimes of behavior separated by a critical doping value of $x=0.22$. Samples with $x \geq 0.22$, C_p exhibits a large λ -like anomaly at T_C and a sharp well-defined critical scattering peak in SANS. Both these characteristics reflect conventional ferromagnetism. On the other hand, these features are either very weak or absent in the lower doping region $x < 0.22$. From the detailed analysis and comparison, they have shown that the magnetoelectronic phase separation occurs only in the doping range $0.04 < x < 0.22$. This range of doping for phase separation in single crystals is narrower as compared to polycrystalline samples.^{1,13,16} The upper range of doping for phase separation is also close to the theoretical prediction. Based on the density-functional-theory calculations, it has been shown that the phase separation occurs only below $x=0.20$.²⁶ Thus the absence of microscopic phase separation in our sample is consistent with these results. The upper inset of Fig. 1(a) represents the inverse susceptibility $\chi^{-1}(=H/M)$ as a function of temperature. This figure shows that $\chi^{-1}(T)$ does not obey the Curie-Weiss law over the entire temperature range above T_C . χ^{-1} deviates from linear behavior around 240 K which is much higher than T_C and exhibits an upward curvature below this temperature. This behavior indicates the presence of critical fluctuations above T_C .

The temperature dependence of resistivity (ρ) of the studied sample is shown in Fig. 1(b). ρ is metallic ($d\rho/dT > 0$) over the whole temperature range and does not show any upturn at low temperatures. In the paramagnetic state, ρ decreases approximately linearly with T . A change in slope at T_C , as a result of spin-disorder scattering, is clearly seen. Below T_C , ρ decreases faster than linear in T . Resistivity of the present sample is small and the value of resistivity ratio $\rho(300 \text{ K})/\rho(15 \text{ K})$ is about 4.5. These values are comparable to those reported for good quality single crystals.¹⁰ As the sharpness of the transition is an indication of sample homogeneity, we have plotted both dM/dT and $d\rho/dT$ as a function of T [inset of Fig. 1(b)]. dM/dT exhibits a sharp and almost symmetric peak at 225.3 K with full width at half-maximum 5 K. In contrary, $d\rho/dT$ exhibits a sharp λ -like peak at 223.2 K. The λ -like peak in $d\rho/dT$ indicates the effect of critical spin fluctuations on resistivity. Similar behavior has also been reported for single crystal with $x=0.30$ where the resistive peak appears slightly below the magnetic one.¹⁰ On the other hand, the peak temperature of $d\rho/dT$ is about 11.6 K higher than the T_C determined from magnetization data for polycrystalline sample with $x=0.30$.²²

Figure 2 shows a series of M vs H isotherms in the vicinity of the Curie temperature. These isotherms show a gradual transition between ferromagnetism and paramagnetism. In order to determine the critical exponents as well as T_C and to understand the nature of magnetic phase transition, we have used a conventional technique known as Arrott method, plotting M^2 vs H/M .²⁷ The positive slope of M^2 vs H/M isotherms in Fig. 3 suggests that the FM-PM phase transition in this compound is second order, which is in agreement with earlier reports.^{22,23} Also, according to the mean-field theory, M^2 vs H/M at various temperatures near T_C should form a progression of parallel lines and the line at $T=T_C$ should pass

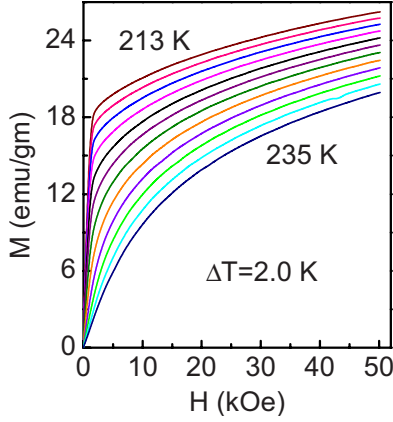


FIG. 2. (Color online) Isothermal magnetization (M vs H) curves at temperatures around T_C of $\text{La}_{0.67}\text{Sr}_{0.33}\text{CoO}_3$.

through the origin. In the present case, the curves in the Arrott plot show a considerable downward curvature even in the high-field region similar to that observed in other conventional FM metals, such as Ni.²⁸ This fact itself implies that the mean-field theory is not valid. Hence, we have analyzed the data according to the modified Arrott plot, based on the Arrott-Noaks equation of state, given by²⁹

$$(H/M)^{1/\gamma} = a \left(\frac{T - T_C}{T_C} \right) + bM^{1/\beta}, \quad (6)$$

where a and b are considered to be constants.

Figure 4 shows the modified Arrott plot, $M^{1/\beta}$ versus $(H/M)^{1/\gamma}$, following Eq. (6). Except at low fields, the isotherms are almost parallel straight lines which are obtained by proper choice of β and γ . The values of β and γ correspond to that of optimum fitting obtained from Eqs. (1) and (2) using a self-consistent method.²² For this, the starting values of $M_S(T)$ and $\chi_0^{-1}(T)$ were determined from the high-field data in Arrott plot (Fig. 3). The calculated values of β and γ were then used to construct new modified Arrott plot

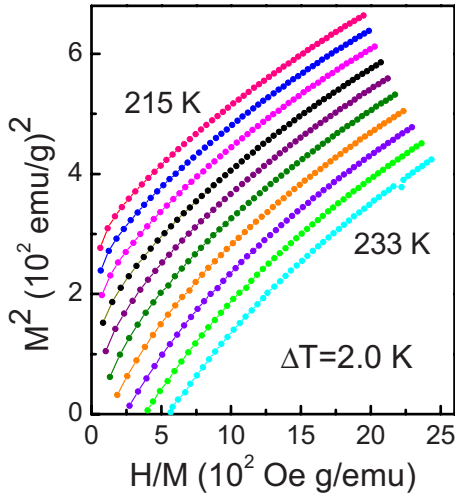


FIG. 3. (Color online) Arrott plot (isotherms of M^2 vs H/M) of $\text{La}_{0.67}\text{Sr}_{0.33}\text{CoO}_3$ at different temperatures close to the Curie temperature ($T_C = 223.0$ K).

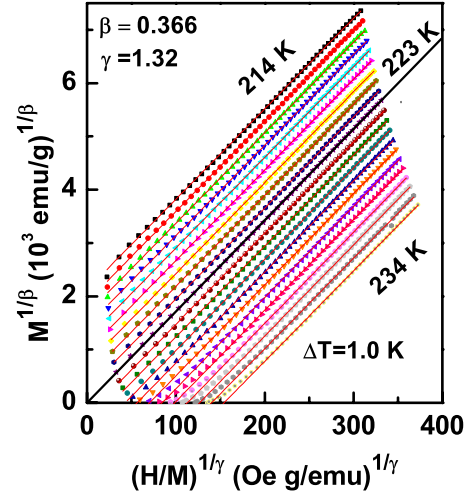


FIG. 4. (Color online) Modified Arrott plot [$M^{1/\beta}$ vs $(H/M)^{1/\gamma}$] isotherms of $\text{La}_{0.67}\text{Sr}_{0.33}\text{CoO}_3$. Solid lines are the high field linear fit to the isotherms. The isotherm (at 223.0 K) close to the Curie temperature ($T_C = 223.0$ K) almost passes through the origin in this plot.

and this process was repeated several times until the iterations converge, leading to optimum fitting values. It may be noted that while fitting the data in Eqs. (1) and (2), the free parameter T_C is varied in order to obtain the best fit results. At low fields, the isotherms are slightly curved, since they are averaged over several domains which are magnetized in different directions. We may compare the quality of fit of the present data on single crystal to those reported for polycrystalline samples. For single crystal, $M^{1/\beta}$ is linear over a wider range of $(H/M)^{1/\gamma}$ as compared to those for polycrystalline samples.^{22,23} Close inspection reveals that unlike single crystal the $M^{1/\beta}$ vs $(H/M)^{1/\gamma}$ plots for polycrystalline samples exhibit a small downward curvature and are slightly off-parallel. Also, the fluctuations in the data are relatively larger in the case of polycrystalline samples. These factors may affect the values of critical exponents.

Figure 5 shows the finally obtained M_S and χ_0^{-1} as a function of temperature. With these values of M_S and χ_0^{-1} , Eq. (1) yields $\beta = 0.363 \pm 0.002$, $T_C = 223.01 \pm 0.01$ K and Eq. (2) yields $\gamma = 1.315 \pm 0.001$, $T_C = 223.00 \pm 0.03$ K. These values of critical exponents and T_C are in good agreement with the values obtained from the modified Arrott plot in Fig. 4 ($\beta = 0.366$, $\gamma = 1.32$, and $T_C = 223.0$ K). The more accurate values of critical exponents as well as T_C are obtained using the Kouvel-Fisher technique where $M_S(dM_S/dT)^{-1}$ and $\chi_0^{-1}(d\chi_0^{-1}/dT)^{-1}$ plotted against temperature should be straight lines with slopes $1/\beta$ and $1/\gamma$, respectively.²⁸ The linear fits to the plots (Fig. 6) yield the values of exponents and T_C are $\beta = 0.361 \pm 0.007$, $T_C = 222.95 \pm 0.07$ K and $\gamma = 1.310 \pm 0.001$, $T_C = 223.00 \pm 0.05$ K. In order to determine the exponent δ , we have opted the $M(H)$ plot at $T = 223$ K, the nearest one to the critical isotherm. Figure 7 shows the critical isotherm $M(H, T = 223.0$ K) vs H plot. The inset shows the same plot in log-log scale. The linear fit to data (the inset of Fig. 7) yields $\delta = 4.64 \pm 0.01$. Using the scaling relation $\delta = 1 + \frac{\gamma}{\beta}$ and the values of β and γ (determined from Figs. 5 and 6), we obtain $\delta = 4.62 \pm 0.01$ and $\delta = 4.61 \pm 0.04$,

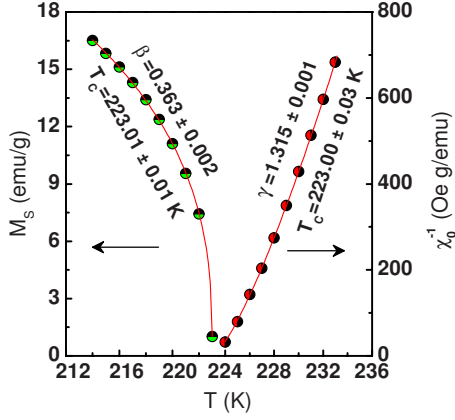


FIG. 5. (Color online) Temperature variation in spontaneous magnetization $M_S(T)$ and inverse initial susceptibility $\chi_0^{-1}(T)$ along with the fit (solid lines) obtained with the help of power law due to Eqs. (1) and (2), which give the values of the exponents and T_C mentioned in the plot.

respectively. These values of δ are close to that obtained from critical isotherm in Fig. 7. So, we can conclude that the values of different critical exponents and T_C determined for $\text{La}_{0.67}\text{Sr}_{0.33}\text{CoO}_3$ single crystal using modified Arrott plots are self-consistent and reasonably accurate within the experimental limits.

To further verify the values of the critical exponents and T_C , we have checked whether these critical exponents can generate a scaling equation of state for this system as given by Eq. (5). Using the values of critical exponents β and γ , and the critical temperature T_C obtained from the Kouvel-Fisher plot, we have constructed the scaled m vs scaled h plot in Fig. 8. The inset of Fig. 8 depicts the same plot on log-log scale. It is clear from the plots that all the data collapse onto two different curves: one below T_C and another above T_C . This suggests that the exponents and T_C are reasonably accurate and unambiguous. For comparison, the values of the critical exponents for the present sample, viz., single crystalline $\text{La}_{0.67}\text{Sr}_{0.33}\text{CoO}_3$, polycrystalline $\text{La}_{0.70}\text{Sr}_{0.30}\text{CoO}_3$ reported by Mira *et al.*,²² polycrystalline

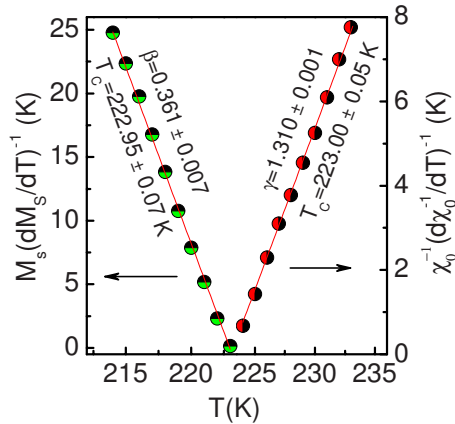


FIG. 6. (Color online) Kouvel-Fisher plot of spontaneous magnetization $M_S(T)$ and inverse initial susceptibility $\chi_0^{-1}(T)$. Solid lines are due to the linear fitting of the data. The exponents and T_C are estimated from the linear fit in this plot.

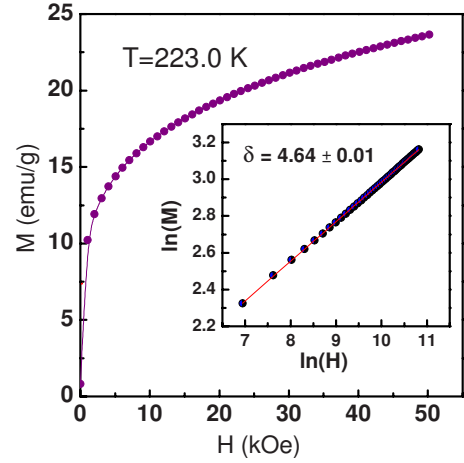


FIG. 7. (Color online) Critical isotherm of M vs H close to the Curie temperature ($T_C = 223.0$ K). Inset shows the same on log-log scale and the straight line is the linear fit following Eq. (3). The critical exponent δ is obtained from the slope of the linear fit.

$\text{La}_{0.50}\text{Sr}_{0.50}\text{CoO}_3$ reported by Mukherjee *et al.*,²³ conventional ferromagnet Ni,^{30,31} and the theoretical values³²⁻³⁵ obtained from different models are given in Table I.

For a homogeneous magnet, the universality class of the magnetic phase transition depends on the range of exchange interaction $J(r)$.³⁶ A renormalization group theory analysis for such systems by Fisher *et al.*³⁶ suggests $J(r) = 1/r^{d+\sigma}$, where d is the dimension of the system and σ is the range of exchange interaction. If σ is greater than two, i.e., $J(r)$ decreases with distance r faster than r^{-5} , the 3D Heisenberg exponents ($\beta = 0.365$, $\gamma = 1.386$, and $\delta = 4.8$) are valid. And the mean-field exponents ($\beta = 0.5$, $\gamma = 1.0$, and $\delta = 3$) hold if $J(r)$ decreases with r slower than $r^{-4.5}$. In the intermediate range, i.e., for $J(r) \approx r^{-3-\sigma}$ with $3/2 \leq \sigma \leq 0.3$, the exponents belong to a different universality class which depends upon σ . We have already mentioned that Mira *et al.*²² reported the

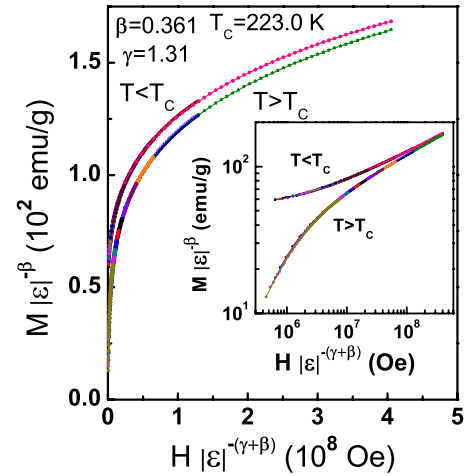


FIG. 8. (Color online) Scaled magnetization of $\text{La}_{0.67}\text{Sr}_{0.33}\text{CoO}_3$ below and above T_C , using β and γ mentioned in the text. This plot shows that all the data collapse onto two different curves: one below T_C and another above T_C . Inset shows the same plot on a log scale. $\varepsilon = (T - T_C)/T_C$ is the reduced temperature.

TABLE I. Comparison of critical parameters of $\text{La}_{0.67}\text{Sr}_{0.33}\text{CoO}_3$ with earlier reports, conventional ferromagnet Ni, and different theoretical models.

Composition	Ref.	Technique	T_C (K)	β	γ	δ
$\text{La}_{0.67}\text{Sr}_{0.33}\text{CoO}_3$	This work	Modified Arrott plot	223.0	0.363 ± 0.002	1.315 ± 0.001	4.62 ± 0.01
		Kouvel-Fisher method		0.361 ± 0.007	1.31 ± 0.001	4.61 ± 0.04
		Critical isotherm				4.64 ± 0.01
$\text{La}_{0.70}\text{Sr}_{0.30}\text{CoO}_3$	22	Modified Arrott plot	223.4	0.43	1.43	4.38
$\text{La}_{0.50}\text{Sr}_{0.50}\text{CoO}_3$	23	Modified Arrott plot	223.0	0.365	1.336	4.66
		Kouvel-Fisher method		0.321	1.351	5.2
		Critical isotherm				4.39
Ni	30 and 31		627.4	0.378 ± 0.004	1.34 ± 0.01	4.58 ± 0.05
3D Heisenberg model	32–35	Theory		0.365	1.386	4.8
MF Theory	32–35	Theory		0.5	1.0	3.0
3D Ising model	32–35	Theory		0.325	1.241	4.82

values of critical exponents for the polycrystalline $\text{La}_{1-x}\text{Sr}_x\text{CoO}_3$ samples in the concentration range $0.2 \leq x \leq 0.3$. Their study reveals that γ corresponds to Heisenberg model but β is mean-field-like. It appears from their results that the polycrystalline $\text{La}_{0.70}\text{Sr}_{0.30}\text{CoO}_3$ does not completely belong to a 3D Heisenberg universality class. However, they explained this unusual behavior of β on the basis of 3D Heisenberg model taking into account the role of nonmagnetic impurity. According to them, the presence of hole-poor diamagnetic matrix of Co^{3+} ion will dilute the magnetic lattice and prevent the occurrence of global long-range magnetic ordering in polycrystalline samples and could lead to a high value of β even in the frame work of Heisenberg model. As another reason for the high value of β , they have cited the role of structural phase transition at T_C . It has been argued that due to the alteration of the Co-O bond length at T_C , the spin-state transition of Co^{3+} ions may show a significant change at T_C . This, in turn, affect β and γ in different ways because the former is calculated from the magnetization data below T_C whereas the later is calculated above T_C . From Table I, one can see that in contrast to the values of the critical exponents reported by Mira *et al.*²² our estimated values of the critical exponents are very close to that for Ni, which is a 3D Heisenberg ferromagnet. Mukherjee *et al.*²³ have studied the critical exponent in the extreme FM limit $\text{La}_{0.5}\text{Sr}_{0.5}\text{CoO}_3$. They have reported $0.321 \leq \beta \leq 0.365$, $1.336 \leq \gamma \leq 1.351$, and $4.39 \leq \delta \leq 4.66$. In contrast to Mira *et al.*, however, they have suggested that the hole-poor matrix brings the values of the critical exponents closer to that for Heisenberg model rather than the mean-field one. The nature of critical fluctuations in $\text{La}_{0.5}\text{Sr}_{0.5}\text{CoO}_3$ has also been analyzed by Menyuk *et al.*²⁴ and observed a very different behavior. They found that the value of γ is close the 3D Ising system but δ is close to the mean-field one. We believe that the above mentioned differences are possibly due to the inhomogeneous nature of polycrystalline samples in the microscopic scale. The sharp FM transition, the absence of linear field-dependent part in magnetization and the higher value of saturation magnetization suggest that the amount of hole-poor matrix is quite small in the present sample, i.e., the

single crystal is more or less magnetically homogeneous.

Whether the ferromagnetism in cobaltites is mediated by double-exchange mechanism as in the case of manganites or not, we can compare and contrast the present result on critical behavior with those reported for manganites. Apart from the microscopic origin of magnetism and spin-state transition, there is another important difference between these two systems which might affect the scaling behavior. The presence of half-filled t_{2g} level core spin and strong Hund's coupling suggest that manganites can be better described in terms of localized or ionic magnetic model. On the other hand, the higher conductivity in the FM phase as well as in the PM phase, the lack of discontinuities in the transport properties at T_C and the absence of colossal magnetoresistance effect are the indications of bandlike ferromagnetism in cobaltites. The spin-density-functional calculations also suggest that hole doping in this material enhances hybridization between cobalt and oxygen ions, reducing ionic character.³⁷ Unlike cobaltites, there are extensive studies on the critical behavior in both single and polycrystalline samples of manganites.^{38–49} The bulk magnetic measurements, except in the close vicinity of the transition, show that the values of the critical exponents for single crystals are close to the theoretically predicted for 3D Heisenberg ferromagnets.^{40–46} However, a diversity in the values of the critical exponents is observed for polycrystalline samples. The values belong to different universality classes like mean-field, 3D Ising and 3D Heisenberg.^{46–50} These differences possibly reflecting the polycrystalline nature of the sample and may be attributed to the different preparation techniques. Normally, the average grain size in polycrystalline samples is small and sensitive to the preparation condition. As the temperature approaches closer to T_C , the correlation length ξ exceeds the grain size, therefore, the fluctuation effects will be replaced by the mean-field behavior. However, due to the larger size of the crystallites in single crystals, the reduced-temperature range ε where one may observe a mean-field behavior is extremely small and beyond the access of these experiments. In spite of several important differences between cobaltites and manganites, it appears that both the systems belong to 3D Heisenberg ferromagnet.

V. CONCLUSION

In conclusion, we have comprehensively studied the critical phenomenon at the FM-PM phase transition in a high-quality single crystal of $\text{La}_{0.67}\text{Sr}_{0.33}\text{CoO}_3$ by dc magnetization. The study suggests that this transition is second order in nature. The values of the critical exponents β , γ , and δ as well as T_C are estimated using various techniques like modified Arrott plot, Kouvel-Fisher plot, and critical isotherm analysis. The values of the critical exponents are in good agreement with those of the theoretically predicted for 3D Heisenberg model and conventional ferromagnet Ni. With

these values of the critical exponents; magnetization-field-temperature (M - H - T) data below and above T_C scale with a single equation of state. This further implies that the obtained critical exponents as well as critical temperature are unambiguous and intrinsic to the system.

ACKNOWLEDGMENTS

The authors would like to thank D. Vieweg for technical help and P. Choudhury and D. Bhoi for useful discussions. We acknowledge the financial support from DFG and INSA.

- ¹M. A. Señaris-Rodríguez and J. B. Goodenough, *J. Solid State Chem.* **116**, 224 (1995); **118**, 323 (1995).
- ²K. Asai, O. Yokokura, N. Nishimori, H. Chou, J. M. Tranquada, G. Shirane, S. Higuchi, Y. Okajima, and K. Kohn, *Phys. Rev. B* **50**, 3025 (1994).
- ³M. W. Haverkort, Z. Hu, J. C. Cezar, T. Burnus, H. Hartmann, M. Reuther, C. Zobel, T. Lorenz, A. Tanaka, N. B. Brookes, H. H. Hsieh, H.-J. Lin, C. T. Chen, and L. H. Tjeng, *Phys. Rev. Lett.* **97**, 176405 (2006).
- ⁴R. Lengsdorf, J.-P. Rueff, G. Vankó, T. Lorenz, L. H. Tjeng, and M. M. Abd-Elmeguid, *Phys. Rev. B* **75**, 180401(R) (2007).
- ⁵T. Vogt, J. A. Hriljac, N. C. Hyatt, and P. Woodward, *Phys. Rev. B* **67**, 140401(R) (2003).
- ⁶R. Lengsdorf, M. Ait-Tahar, S. S. Saxena, M. Ellerby, D. I. Khomskii, H. Micklitz, T. Lorenz, and M. M. Abd-Elmeguid, *Phys. Rev. B* **69**, 140403(R) (2004).
- ⁷S. Yamaguchi, Y. Okimoto, and Y. Tokura, *Phys. Rev. B* **55**, 8666 (1997).
- ⁸I. Fita, R. Szymczak, R. Puzniak, I. O. Troyanchuk, J. Fink-Finowicki, Ya. M. Mukovskii, V. N. Varyukhin, and H. Szymczak, *Phys. Rev. B* **71**, 214404 (2005).
- ⁹M. Kriener, C. Zobel, A. Reichl, J. Baier, M. Cwik, K. Berggödl, H. Kierspel, O. Zabara, A. Freimuth, and T. Lorenz, *Phys. Rev. B* **69**, 094417 (2004).
- ¹⁰H. M. Aarbogh, J. Wu, L. Wang, H. Zheng, J. F. Mitchell, and C. Leighton, *Phys. Rev. B* **74**, 134408 (2006).
- ¹¹K. Mydeen, P. Mandal, D. Prabhakaran, and C. Q. Jin, *Phys. Rev. B* **80**, 014421 (2009).
- ¹²M. Paraskevopoulos, J. Hemberger, A. Krimmel, and A. Loidl, *Phys. Rev. B* **63**, 224416 (2001).
- ¹³J. Wu and C. Leighton, *Phys. Rev. B* **67**, 174408 (2003), and references therein.
- ¹⁴P. Mandal, A. Hassen, and P. Choudhury, *J. Appl. Phys.* **100**, 103912 (2006); P. Mandal, P. Choudhury, S. K. Biswas, and B. Ghosh, *Phys. Rev. B* **70**, 104407 (2004).
- ¹⁵Z. Jirák, J. Hejtmanek, K. Knížek, and M. Veverka, *Phys. Rev. B* **78**, 014432 (2008).
- ¹⁶P. L. Kuhns, M. J. R. Hoch, W. G. Moulton, A. P. Reyes, J. Wu, and C. Leighton, *Phys. Rev. Lett.* **91**, 127202 (2003).
- ¹⁷C. He, S. Eisenberg, C. Jan, H. Zheng, J. F. Mitchell, and C. Leighton, *Phys. Rev. B* **80**, 214411 (2009).
- ¹⁸C. He, S. El-Khatib, J. Wu, J. W. Lynn, H. Zheng, J. F. Mitchell, and C. Leighton, *EPL* **87**, 27006 (2009).
- ¹⁹C. He, M. A. Torija, J. Wu, J. W. Lynn, H. Zheng, J. F. Mitchell, and C. Leighton, *Phys. Rev. B* **76**, 014401 (2007).
- ²⁰R. X. Smith, M. J. R. Hoch, P. L. Kuhns, W. G. Moulton, A. P. Reyes, G. S. Boebinger, J. Mitchell, and C. Leighton, *Phys. Rev. B* **78**, 092201 (2008).
- ²¹H. Eugene Stanley, *Introduction to Phase Transitions and Critical Phenomena* (Oxford University Press, New York, 1971).
- ²²J. Mira, J. Rivas, M. Vázquez, J. M. García-Beneytez, J. Arcas, R. D. Sánchez, and M. A. Señaris-Rodríguez, *Phys. Rev. B* **59**, 123 (1999).
- ²³S. Mukherjee, P. Raychaudhuri, and A. K. Nigam, *Phys. Rev. B* **61**, 8651 (2000).
- ²⁴N. Menyuk, P. M. Raccach, and K. Dwight, *Phys. Rev.* **166**, 510 (1968).
- ²⁵D. Prabhakaran, A. T. Boothroyd, F. R. Wondre, and T. J. Prior, *J. Cryst. Growth* **275**, e827 (2005).
- ²⁶K. Knížek, Z. Jirák, J. Hejtmanek, and P. Novák, *J. Magn. Magn. Mater.* **322**, 1221 (2010).
- ²⁷A. Arrott, *Phys. Rev.* **108**, 1394 (1957).
- ²⁸J. S. Kouvel and M. E. Fisher, *Phys. Rev.* **136**, A1626 (1964).
- ²⁹A. Arrott and J. E. Noakes, *Phys. Rev. Lett.* **19**, 786 (1967).
- ³⁰J. S. Kouvel and D. S. Rodbell, *Phys. Rev. Lett.* **18**, 215 (1967).
- ³¹L. P. Kadanoff, W. Götze, D. Hamblen, R. Hecht, E. A. Lewis, V. V. Palciauskas, M. Rayl, J. Swift, D. Aspnes, and J. Kane, *Rev. Mod. Phys.* **39**, 395 (1967), and references therein.
- ³²S. N. Kaul, *J. Magn. Magn. Mater.* **53**, 5 (1985).
- ³³M. Seeger, S. N. Kaul, H. Kronmüller, and R. Reisser, *Phys. Rev. B* **51**, 12585 (1995).
- ³⁴C. Bagnuls and C. Bervillier, *Phys. Rev. B* **32**, 7209 (1985).
- ³⁵V. Privman, P. C. Hohenberg, and A. Aharony, in *Phase Transitions and Critical Phenomena*, edited by C. Domb and J. L. Lebowitz (Academic, New York, 1991), p. 1.
- ³⁶M. E. Fisher, S. K. Ma, and B. G. Nickel, *Phys. Rev. Lett.* **29**, 917 (1972).
- ³⁷P. Ravindran, H. Fjellvag, A. Kjekshus, P. Blaha, K. Schwarz, and J. Luitz, *J. Appl. Phys.* **91**, 291 (2002).
- ³⁸K. Ghosh, C. J. Lobb, R. L. Greene, S. G. Karabashev, D. A. Shulyatev, A. A. Arsenov, and Y. Mukovskii, *Phys. Rev. Lett.* **81**, 4740 (1998).
- ³⁹D. Kim, B. L. Zink, F. Hellman, and J. M. D. Coey, *Phys. Rev. B* **65**, 214424 (2002).
- ⁴⁰S. Nair, A. Banerjee, A. V. Narlikar, D. Prabhakaran, and A. T. Boothroyd, *Phys. Rev. B* **68**, 132404 (2003).
- ⁴¹M. Sahana, U. K. Rössler, N. Ghosh, S. Elizabeth, H. L. Bhat, K. Dörr, D. Eckert, M. Wolf, and K.-H. Müller, *Phys. Rev. B* **68**,

- 144408 (2003).
- ⁴²W. Li, H. P. Kunkel, X. Z. Zhou, G. Williams, Y. Mukovskii, and D. Shulyatev, *Phys. Rev. B* **70**, 214413 (2004).
- ⁴³B. Padmanabhan, H. L. Bhat, S. Elizabeth, S. Rössler, U. K. Rössler, K. Dörr, and K. H. Müller, *Phys. Rev. B* **75**, 024419 (2007).
- ⁴⁴W. Jiang, X. Z. Zhou, G. Williams, Y. Mukovskii, and K. Glazyrin, *Phys. Rev. B* **77**, 064424 (2008).
- ⁴⁵P. Sarkar, S. Arumugam, P. Mandal, A. Murugeswari, R. Thiagarajan, S. Esaki Muthu, D. Mohan Radheep, C. Ganguli, K. Matsubayshi, and Y. Uwatoko, *Phys. Rev. Lett.* **103**, 057205 (2009).
- ⁴⁶J. Yang, Y. P. Lee, and Y. Li, *Phys. Rev. B* **76**, 054442 (2007), and references therein.
- ⁴⁷Ch. V. Mohan, M. Seeger, H. Kronmüller, P. Murugaraj, and J. Maier, *J. Magn. Magn. Mater.* **183**, 348 (1998).
- ⁴⁸S. Taran, B. K. Chaudhuri, S. Chatterjee, H. D. Yang, S. Neeleshwar, and Y. Y. Chen, *J. Appl. Phys.* **98**, 103903 (2005).
- ⁴⁹A. K. Pramanik and A. Banerjee, *Phys. Rev. B* **79**, 214426 (2009).
- ⁵⁰J. Fan, L. Ling, B. Hong, L. Zhang, L. Pi, and Y. Zhang, *Phys. Rev. B* **81**, 144426 (2010).